

# Investigation on Formation Mechanism of Magnetic Nanoparticles-Coated on Polystyrene Microspheres in Aqueous Solution of Anhydrous Ethylenediamine and Hexamethylenetetramine

Mingjuan Han<sup>1</sup>, Yanyan Wei<sup>1</sup>, Mingyue Chen<sup>1</sup>, Ying Li<sup>1</sup>, Jikui Wang<sup>1\*</sup>, Lihong Dong<sup>2</sup>

<sup>1</sup>College of Chemistry and Molecular Engineering, Nanjing Tech University, Nanjing, 210009, PR China

<sup>2</sup>Department of Chemistry, Tonghua Normal College, Tonghua 134002, PR China

\*Corresponding author: Jikui Wang, College of Chemistry and Molecular Engineering, Nanjing Tech University, Nanjing, 210009, PR China, Tel: +13-951-945-201; E-mail: [njwjk@163.com](mailto:njwjk@163.com)

## Abstract

The monodispersed polystyrene (PS) microspheres were modified by concentrated sulfuric acid to obtain PS microspheres with negative charges, and then polystyrene/magnetic composite microspheres were fabricated by a simple and novel method in aqueous solution of anhydrous Ethylene diamine (EDA) and Hexamethylenetetramine (HMTA). Through serials of contrast experiments (based on different precursor ratios) and characteristic investigations of target samples, we have discovered the functions of EDA and HMTA, respectively. EDA not only acted as a weak base providing OH<sup>-</sup> ions, but also acted as a chelating combining with Fe<sup>2+</sup> ions, which could control the concentration of Fe<sup>2+</sup> ions, and resulted in the pure Fe<sub>3</sub>O<sub>4</sub> nanoparticle coated on the surface of PS microspheres. Otherwise, the typical XRD peaks of FeOOH and Fe<sub>3</sub>O<sub>4</sub> appeared, simultaneously, if HMTA played an action in the formation magnetic nanoparticles-coated PS microspheres. It indicated that HMTA could provide OH<sup>-</sup> ions and make Fe<sup>2+</sup> to become FeOOH and Fe<sub>3</sub>O<sub>4</sub>, simultaneously, which could be confirmed the reaction mechanism suggested by us. Finally, the corresponding possible reaction mechanisms of EDA and HMTA for fabricating magnetic composite microspheres have been suggested in detail by combining SEM, XRD, FTIR analysis together.

Received date: March 08, 2017

Accepted date: April 18, 2017

Published date: April 25, 2017

**Citation:** Jikui Wang., et al. Investigation on Formation Mechanism of Magnetic Nanoparticles-Coated on Polystyrene Microspheres in Aqueous Solution of Anhydrous Ethylenediamine and Hexamethylenetetramine. (2017) J Nanotechnol Mater Sci 4(1): 27- 31.

DOI: 10.15436/2377-1372.17.1406



**Keywords:** PS/Fe<sub>3</sub>O<sub>4</sub>; Magnetic composite microspheres; Anhydrous Ethylenediamine (EDA); Formation mechanism.

## Introduction

In the past decades, there is a growing interest in the design and synthesis of composite microspheres with a dielectric solid sphere (e.g., silica, polystyrene) covered by metallic and their corresponding metal oxides shell, such as copper<sup>[1]</sup>, gold<sup>[2]</sup>, silver<sup>[3,4]</sup>, iron oxide<sup>[5]</sup>, zinc oxide<sup>[6,7]</sup>, titanium oxide<sup>[8,9]</sup> and zirconium dioxide<sup>[10]</sup>. Such materials may exhibit a few unique electrical, optical, magnetic, catalytic, well-dispersed, or mechanical properties comparing to the traditional isotropic spherical microspheres. Iron oxide, which is a typical super paramagnetic material possessing a cubic inverse spinel structure, has been widely investigated due to their potential applications such as catalysts<sup>[11]</sup>, photonics<sup>[12]</sup>, separation and purification of bio-molecules, MRI contrast agent, hyperthermia, biosensor, and tar-

geted drug delivery<sup>[13-16]</sup>. Owing to these properties of magnetic nanoparticles, the design and fabrication of various composite microspheres architectures based on magnetic nanoparticles has become an important research subject.

Polymer-based magnetic composite materials have their advantageous characteristics combining properties of easily synthesizing and modifying, and solving the problem of condensation of magnetic microspheres. In the system of Fe<sup>2+</sup>, Fe<sup>3+</sup> in ammonium hydroxide (NH<sub>3</sub>•H<sub>2</sub>O) solution and tetramethyl ammonium hydroxide ((CH<sub>3</sub>)<sub>4</sub>NOH) solution, monodisperse super paramagnetic PS/iron oxide composite colloidal spheres were fabricated in 2001 by Xu<sup>[17]</sup>. Later, Tang and co-workers<sup>[18,19]</sup> have reported a novel method of fabricating PS/magnetic materials composite particles in Hexamethylenetetramine(HMTA)/Diethylene glycol (DEG) solution, the effects of DEG in aqueous



solutions on morphology and texture of the magnetite composite PS microspheres produced from a forced hydrolysis reaction  $\text{FeCl}_2$  solution were investigated. Then, Fang and co-workers<sup>[20]</sup> fabricated a novel PS/ $\text{Fe}_3\text{O}_4$  composite microspheres by means of porous morphology of the PS obtained by etching silica particles and investigated their magnetorheology in 2009. Recently, PS/ $\text{Fe}_3\text{O}_4$  composites<sup>[21]</sup> were fabricated through mini emulsion and emulsion polymerization conventional techniques using different stabilizers and ferrofluids stabilized using the mixture of anionic/nonionic stabilizer and Acrylic acid (AA). However, up to now, it concludes that the formation mechanism of PS/ $\text{Fe}_3\text{O}_4$  in corresponding systems is few investigated in detail.

In this paper, we emphasized a simple method for the synthesis of PS/ $\text{Fe}_3\text{O}_4$  composite microspheres in anhydrous Ethylenediamine (EDA)/HMTA aqueous solution, and placed the attraction on the possible formation mechanism of PS/ $\text{Fe}_3\text{O}_4$ , especially the formation and reaction mechanism of  $\text{Fe}_3\text{O}_4$  shell. The monodispersed PS microspheres were prepared by dispersion polymerization, and their surfaces were modified by concentrated sulfuric acid to obtain PS microspheres with negative charges, then the PS/ $\text{Fe}_3\text{O}_4$  composite microspheres were prepared without additional oxidizing agent. Through a series of contrast experiments, we have discovered the functions of EDA and HMTA, individually, and investigated the corresponding possible reaction mechanism of the shell of iron compounds and the formation mechanism of PS/ $\text{Fe}_3\text{O}_4$  in detail by the SEM, XRD, IR analysis, respectively.

## Experimental section

### Materials

Styrene, ferrous chloride tetrahydrate ( $\text{FeCl}_2 \cdot 4\text{H}_2\text{O}$ ), anhydrous Ethylene diamine (EDA) and Ethylene glycol (EG) were purchased from Shanghai Lingfeng Chemical Reagent Co. Ltd. (China). Polyvinylpyrrolidone (PVP, K30) was bought from Sinopharm Chemical Reagent Co. Ltd. (China). 2, 2'-azobisisobutyronitrile (AIBN) and Hexamethylenetetramine (HMT) were purchased from Aladdin and J & K, respectively. Sulfuric acid ( $\text{H}_2\text{SO}_4$ , 98%), absolute ethanol were obtained from Shanghai Chemical Reagent Co. (China). It should be noted that all the materials used were without further purification.

### Synthesis of monodispersed PS microspheres and sulfonated PS microspheres

The monodispersed polystyrene (PS) microspheres were fabricated by dispersion polymerization and modified by concentrated sulfuric acid to obtain PS microspheres with negative charges<sup>[22]</sup>. First, the mixture of ethanol, deionized water, PVP was deoxygenated by bubbling nitrogen gas and vigorously stirring for 20 min at 70 °C. After that, styrene (20 mL) and AIBN (0.182 g) were adding to the mixed solution. The polymerization was kept at 70 °C for another 12 h with a continuous stirring under nitrogen atmosphere. After the reaction, the obtained dispersion was centrifuged (5000 rpm) and washed with ethanol for five times. Then, the obtained microspheres were dried in a vacuum oven at 25 °C for 12 h. After drying, about 1.7 g PS powder was sulfonated with 60 mL concentrated sulfuric acid at 40 °C for 12 h<sup>[22]</sup>. When the dispersion liquid cooled down to 25 °C, the sulfonated PS microspheres were purified using the same procedures as these for purifying PS microspheres. Finally, the sulfonated PS microspheres (yellow fine powder) were obtained

after being dried in a vacuum oven at 25 °C.

### Preparation of PS/ $\text{Fe}_3\text{O}_4$ composite microspheres

About 0.2 g sulfonated PS microspheres were dispersed in 120 mL deoxygenated water under ultrasonication. Then, a certain amount of  $\text{FeCl}_2 \cdot 4\text{H}_2\text{O}$ , EDA and HMTA was dissolved in 10 mL deionized water, respectively, and added their aqueous solution into the dispersion in turn. The resulting solution was heated to 80 °C for 5 h. The obtained PS/ $\text{Fe}_3\text{O}_4$  particles were centrifuged (8000 rpm) and washed with ethanol for six times, and then dried in a vacuum oven at 40 °C for 12 h. The detailed reaction conditions were given in Table 1.

## Results and Discussion

### Particle morphology

Mono-disperse and smooth PS microspheres with an average diameter of 1.5  $\mu\text{m}$  were showed in Figure 1(a). Figures 1(b-e) presented that SEM images of magnetic material/PS composite microspheres fabricated by adjusting the mole ratios of  $\text{FeCl}_2 \cdot 4\text{H}_2\text{O}$ /HMTA/EDA. First, it could be observed from Figures 1(b-d) that the complete, homogeneous and needle-like nanoparticles well coated on the surface of PS particles, respectively, when the mole ratios of  $\text{Fe}^{2+}$ /EDA were kept 1:3 (1#-3#), and the SEM images showed that there were no any obvious differences. Otherwise, Figure 1(e) showed that there were few small particles coated on the surface of PS microspheres when the chelating EDA was absent (6# shown in Table 1). It could be concluded that the increasing of moles of HMTA could not change the morphology of composite microspheres, importantly; magnetic material-coated composite microspheres could not be obtained when EDA as a good complexing agent is absent.

**Table 1:** The PS/ $\text{Fe}_3\text{O}_4$  composite microspheres design of experiments.

Sample(#)	$\text{Fe}^{2+}$ /HMTA/EDA (mol)	Iron concentration (mol)
1	1:0:3	0.0011
2	1.5:0:3	0.0017
3	1:2:3	0.0011
4	1.5:2:3	0.0017
5	1:4:3	0.0011
6	1:4:0	0.0011

### Crystal structure of nanoparticles coated on the surface of PS microspheres

In order to investigate whether the nanoparticles coated on the surface of PS are our target  $\text{Fe}_3\text{O}_4$  particles or any other iron species, Figures 2 and 3 showed the XRD patterns of samples 1# - 6# which were prepared by adjusting the different mole ratios of  $\text{Fe}^{2+}$ /HMTA/EDA. First, there were only five diffraction peaks at  $2\theta$  value of 30.2°, 35.6°, 43.3°, 57.3° and 62.9° appeared in XRD patterns of samples 1#, 2# and 3#, which could be indexed to the peaks of the face-centered-cubic phase of  $\text{Fe}_3\text{O}_4$  (JCPDS no.19-629)<sup>[18,19]</sup>, these peaks corresponded to five indexed planes (220), (311), (400), (511), and (440) of magnetite  $\text{Fe}_3\text{O}_4$ , respectively. Furthermore, no characteristic diffraction peaks from other phases or impurities were detected in the XRD patterns of samples 1#, 2# and 3#, which implied that particles coated on the surface of PS were pure  $\text{Fe}_3\text{O}_4$  nanoparticles. Second, comparing with the XRD patterns of

samples 1#, 3# (in Figure 2) and 5# (in Figure 3), we could find that the crystal structure of  $\text{Fe}_3\text{O}_4$  nanoparticles did not change by increasing the mole number of HMTA. However, comparing the XRD patterns of samples 3# and 4#, it could be found the typical peaks of  $\text{FeOOH}$  (showed by arrows) and  $\text{Fe}_3\text{O}_4$  appear (sample 4#), simultaneously, if the mole ratio of  $\text{Fe}^{2+}/\text{EDA}$  was increased more than 1:3 (exactly, it is up to 1.5:3) when the mole ratio of HMTA/EDA was still equal to 2:3 in synthetic system. It indicated that EDA first combined with the  $\text{Fe}^{2+}$ , and then HMTA had the choice to participate in combining with the excess  $\text{Fe}^{2+}$  if the mole ratio of  $\text{Fe}^{2+}/\text{EDA}$  was increased more than 1:3. Third, as shown in Figures 2(a) and (b) (samples 1# and 2#), pure  $\text{Fe}_3\text{O}_4$ -coated PS microspheres could be successfully obtained by one step when only adding EDA (HMTA was absent). It indicates that EDA played a decisive role in forming  $\text{Fe}_3\text{O}_4$  and  $\text{Fe}_3\text{O}_4$ -coated on PS microspheres, which was because EDA could provide

$\text{OH}^-$  ions, meanwhile, EDA had the chelating activity with metals<sup>[23]</sup>. Finally, we talked about HMTA which was a non-toxic, water soluble and non-ionic tetradentate cyclic tertiary amine, furthermore, it served not only as complexing and passivating reagent but also as an indirect soft template<sup>[24]</sup>. Otherwise, there were few magnetic particles coated on the surface of PS, shown in Figure 1(e) when the only HMTA was added into this reaction system (EDA was absent), and then it indicated that HMTA did not play an important role in the formation of composite microspheres. Meanwhile, from the XRD patterns of Figure 3(b), the typical peaks of  $\text{FeOOH}$  (showed by arrows) and  $\text{Fe}_3\text{O}_4$  appear, simultaneously, when only HMTA was added into this reaction system (EDA was absent). It indicated that HMTA can provide  $\text{OH}^-$  ions and make  $\text{Fe}^{2+}$  to become  $\text{FeOOH}$  and  $\text{Fe}_3\text{O}_4$ , simultaneously, which could be confirmed the reaction mechanism suggested by us.

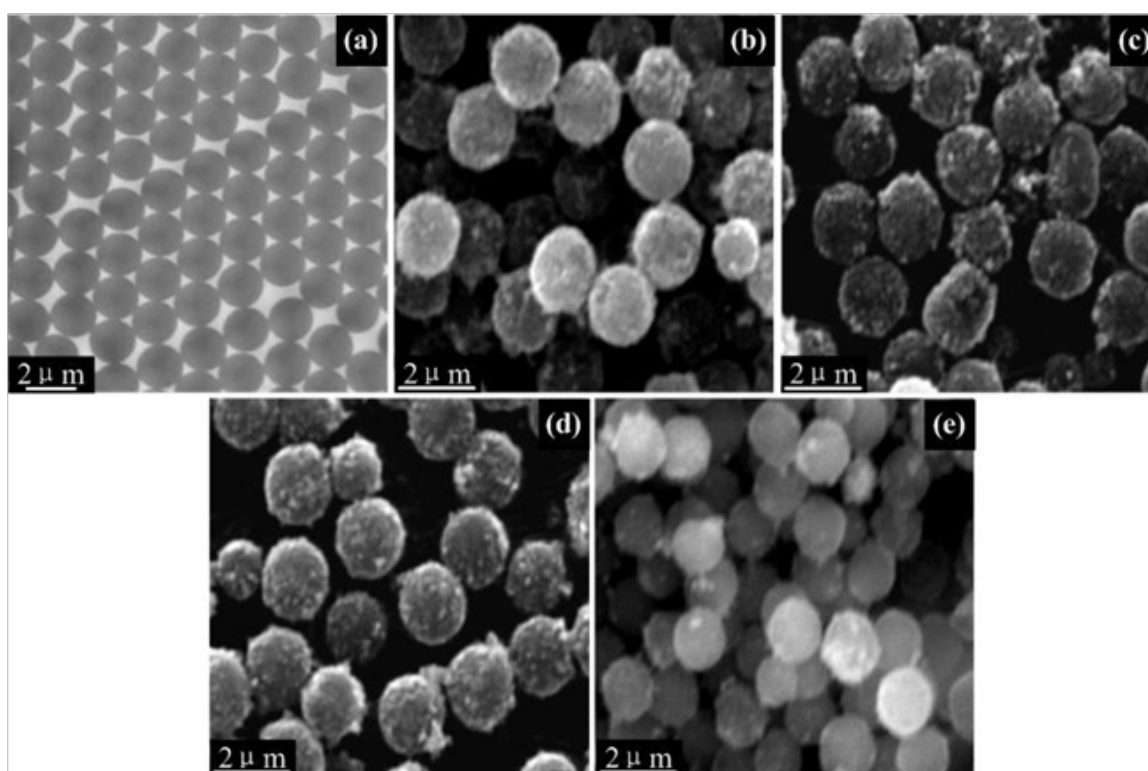


**Figure 1:** TEM image of (a) PS microspheres; SEM images of  $\text{PS}/\text{Fe}_3\text{O}_4$  composite microspheres (b) Sample 1# (1:0:3); (c) Sample 3# (1:2:3), (d) Sample 5# (1:4:3) and (e) Sample 6# (1:4:0).

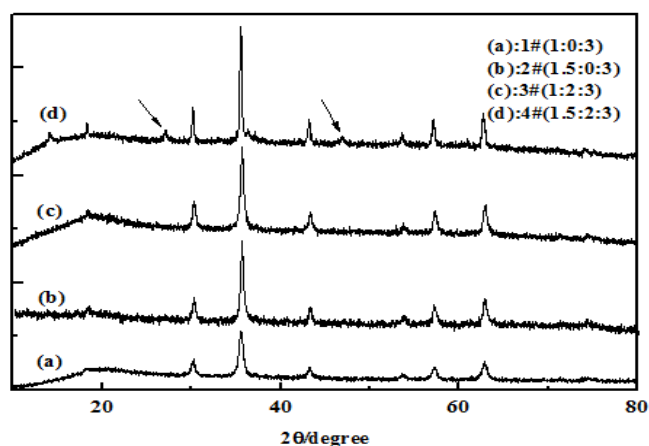


**Figure 2:** (a)-(d) presented the XRD patterns of the samples 1# - 4#, respectively.

According to the experimental results, now, we displayed the reaction mechanisms suggested by us when EDA and HMTA were added into the reaction system, respectively. First, it was well-known that EDA was a good chelating<sup>[23]</sup>, the ferrous-EDA complex ( $[\text{Fe}(\text{EDA})_3]^{2+}$ ) immediately formed (Equation (1)) when the EDA was added according to the mole ratio of  $\text{Fe}^{2+}/\text{EDA}(=1:3)$ . The surface of sulfonated PS microspheres was negative, which led to the increment of polarity of PS surface, then PS microspheres were surrounded by ( $[\text{Fe}(\text{EDA})_3]^{2+}$ ) through electrostatic forces after adding  $\text{Fe}^{2+}$  and EDA in the reaction system, which resulted in that  $\text{Fe}_3\text{O}_4$  successfully coated on the surface of sulfonated PS microspheres. As for the controlled releasing of  $\text{Fe}^{2+}$  ions mentioned above, which was decomposed by the equilibrium of the ferrous-EDA complex (Equation (1)). Meanwhile, the free EDA molecules experienced the hydrolysis process (Equation (2)), which could provide  $\text{OH}^-$

ions. Gradually, the concentrations of  $\text{Fe}^{2+}$  and  $\text{OH}^-$  correspondingly increased, and then formed  $\text{Fe}_3\text{O}_4$  according to Equation (3) when  $\text{O}_2$  in the air existed in this reaction system (Equation (3)). Hence, EDA not only acted as a weak base during the reaction, which could effectively control the supply of  $\text{OH}^-$  ions, but also acted as a chelating combining with  $\text{Fe}^{2+}$  ions, which could control the concentration of  $\text{Fe}^{2+}$  ions.

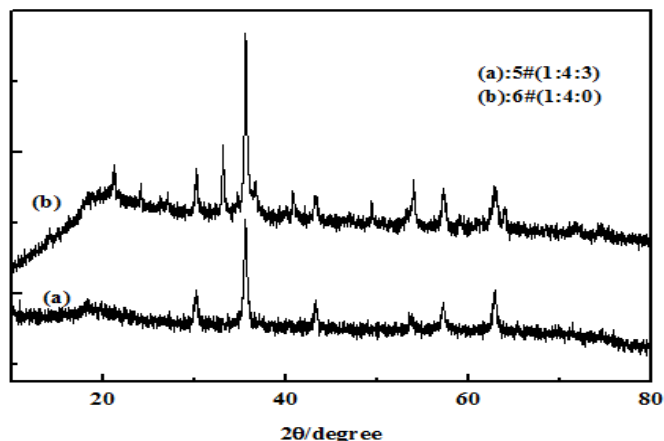
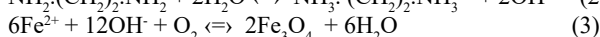
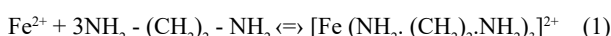
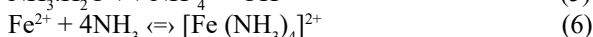
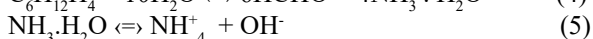


**Figure 3:** (a) and (b) presented the XRD patterns of samples 5# and 6#, respectively.



On the other hand, the reaction mechanism was suggested by us when HMTA did its work in the reaction system. Both  $\text{FeOOH}$  and  $\text{Fe}_3\text{O}_4$  particles could be obtained when only HMTA (sample 6#) was added, which was confirmed from the XRD pattern in Figure 3(b). It meant that HMTA could provide  $\text{OH}^-$  ions by means of hydrolysis (Equations(4) and (5)) and HMTA could serve as a complexing with metal ions as well<sup>[24]</sup>, then the ferrous- $\text{NH}_3$  complex immediately formed by Equation (6) when the HMTA was added. Subsequently, the sulfonated PS microspheres were surrounded by through electrostatic forces in the reaction system, and then the magnetic particles were successfully coated on the surface of PS microspheres. However, it could be observed that few magnetic particles coated on the surface of PS microspheres from TEM in Figure 1(e). It indicated that few formed by Equation (6) and the most of  $\text{Fe}^{2+}$  source appeared by  $\text{Fe}^{2+}$  ions in reactive system. Free  $\text{Fe}^{2+}$  ions could be easily oxidized to  $\text{Fe}^{3+}$  ions in the reaction system, the  $\text{OH}^-$  ions obtained by the hydrolysis of HMTA would react with the oxidized  $\text{Fe}^{3+}$  ions, and then the main product was  $\text{FeOOH}$  and  $\text{Fe}_3\text{O}_4$  particles (Equation (7)). Moreover,  $\text{Fe}_3\text{O}_4$  particles eventually obtained by dehydrating between the  $\text{FeOOH}$  and  $\text{Fe}^{2+}$  ions. Therefore, few magnetic particles could coat on PS microspheres due to the freedom of  $\text{Fe}^{3+}$  ions in solution and the spatial structure of  $[\text{Fe}(\text{NH}_3)_4]^{2+}$  although HMTA could be served as a complexing agent, which was confirmed by TEM of Figure 1(e). The overall reaction equation obtained Equation (9) by combining Equation (7) and Equation (8). Thus, the coated-nanoparticles on PS microspheres were magnetic  $\text{FeOOH}$  and  $\text{Fe}_3\text{O}_4$  when HMTA did its work in the reaction system.



### FTIR spectra of the samples

The structure of the fabricated composite microspheres were further investigated, Figure 4 showed the IR spectra of PS, sulfonated PS microspheres,  $\text{Fe}_3\text{O}_4$  particles and PS/ $\text{Fe}_3\text{O}_4$  composite microspheres. First, as shown in Figure 4, the characteristic peaks in both spectra of PS (Figures 4(a)) and sulfonated PS microspheres (Figures 4(b)) around 697, 756, 1452 and 1493  $\text{cm}^{-1}$  could be clearly observed, which were ascribed to characteristic structure of PS microspheres<sup>[22]</sup>, it indicated that the two samples possessed the PS backbone. Meanwhile, it could be found that the strong peak at 1180  $\text{cm}^{-1}$  was present in Figure 4(b) and absent in Figure 4(a), which was due to the characteristic peak of sulfuric acid groups ( $-\text{SO}_3\text{H}$ ) of sulfonated PS microspheres, all in all, this result demonstrated that the PS spheres had been successfully modified by sulfuric acid groups ( $-\text{SO}_3\text{H}$ ). Second, as shown in IR spectra of  $\text{Fe}_3\text{O}_4$  in Figure 4(c), the broadband at 3422 and 1629  $\text{cm}^{-1}$  illustrated the presence of hydroxyl groups ( $-\text{OH}$ ) on the surface of  $\text{Fe}_3\text{O}_4$ , and bands appeared at 577  $\text{cm}^{-1}$  were attributed to Fe-O vibration<sup>[25]</sup>. Finally, compared with the IR spectra of Figures 4(b)-(d), it showed that the characteristic peaks due to hydroxyl groups on the surface of  $\text{Fe}_3\text{O}_4$  and Fe-O vibration were well displayed in Figure 4(d), mean while, the intensity of these peaks characterized by PS microspheres was weaker, which was because the PS microspheres were surrounded by  $\text{Fe}_3\text{O}_4$  particles. IR spectra showed that the  $\text{Fe}_3\text{O}_4$ -coated PS composite microspheres were successfully synthesized.

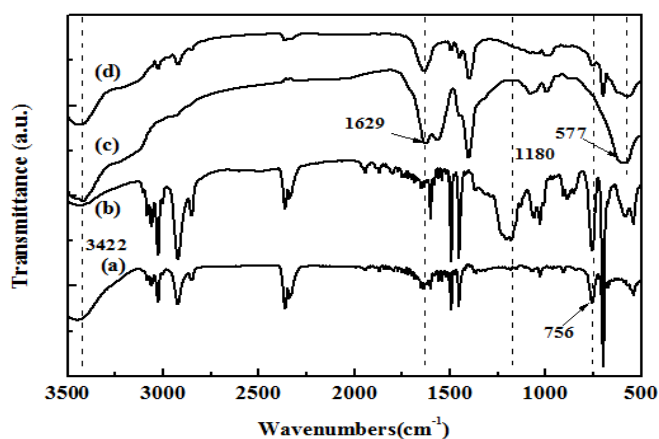


**Figure 4:** (a) FTIR patterns of PS microspheres, (b) Sulfonated PS microspheres, (c)  $\text{Fe}_3\text{O}_4$  nanoparticles and (d) PS/ $\text{Fe}_3\text{O}_4$  composite microspheres.

### Conclusion

In summary, we described a simple, effective, and friendly method to fabricate the polystyrene (PS)/magnetic composite microspheres in aqueous solution of EDA and HMTA. Neither additional oxidizing agent nor any surfactant was necessary in this process. In order to investigate whether the coated nanoparticles of PS was our target  $\text{Fe}_3\text{O}_4$  nanoparticles or any other iron species, the XRD patterns of samples confirmed the formation of PS/ $\text{Fe}_3\text{O}_4$  composite microspheres and the coated nanoparticles was pure  $\text{Fe}_3\text{O}_4$  particles. Through a series of contrast experiments, we have discovered the functions of EDA and

HMTA, respectively, EDA not only acted as a weak base providing OH<sup>-</sup> ions, but also acted as a chelating combining with Fe<sup>2+</sup> ions, which could control the concentration of Fe<sup>2+</sup> ions, and resulted in the pure Fe<sub>3</sub>O<sub>4</sub> particle coated on the surface of PS microspheres. Furthermore, FeOOH and Fe<sub>3</sub>O<sub>4</sub> nanoparticles could be obtained, simultaneously, when only adding HMTA, which was confirmed from the XRD patterns. Meanwhile, it could be observed from TEM analysis that few magnetic particles coated on PS microspheres, the reason for this was due to the freedom of Fe<sup>3+</sup> ions in solution and the spatial structure of [Fe(NH<sub>3</sub>)<sub>4</sub>]<sup>2+</sup>. Finally, the corresponding possible reaction mechanisms of the coated Fe<sub>3</sub>O<sub>4</sub> nanoparticles and PS/Fe<sub>3</sub>O<sub>4</sub> composite microspheres in detail have been suggested and confirmed by comparing SEM, XRD and FTIR analysis together.

### Acknowledgments

This work was financially supported by the Natural Nature Science Foundation of Jiangsu Province (No. BK20131407), Natural Nature Science Foundation of China (Nos. 21003074, 21103126) and 12<sup>th</sup> Five-Year Plan in science and technology of the Education Department of Jilin Province (No.2011305).

**Conflict of Interest:** The authors declare no conflict of interests.

### References

- Heo, Y., Hyun, D., Kumar, M.R., *et al.* Preparation of copper (II) oxide bound on polystyrene beads and its application in the aryl aminations: synthesis of Imatinib. (2012) *Tetrahedron Letters* 53(49): S6657-S6661.  
[Crossref](#) | [Others](#)
- Kandpal, D., Kalele, S., Kulkarni, S.K. Synthesis and characterization of silica-gold core-shell (SiO<sub>2</sub> @ Au) nanoparticles. (2007) *Pramana J Phys* 69(2): S277-S283.  
[Others](#)
- Deng, Z., Zhu, H., Peng, B., *et al.* Synthesis of PS/Ag nanocomposite spheres with catalytic and antibacterial activities. (2012) *ACS Appl Mat Interfaces* 4(10): S5625-S5632.  
[PubMed](#) | [Crossref](#) | [Others](#)
- Chen, D., Liu, H.Y., Liu, J.S., *et al.* A general method for synthesis continuous silver nanoshells on dielectric colloids. (2008) *Thin Solid Films* 516(18): S6371-S6376.  
[Crossref](#) | [Others](#)
- Li, Q.Y., Wang, P.Y., Zhou, Y.L., *et al.* A magnetic mesoporous SiO<sub>2</sub>/Fe<sub>3</sub>O<sub>4</sub> hollow microsphere with a novel network-like composite shell: synthesis and application on laccase immobilization. (2016) *J Sol-Gel Sci Technol* 78(3): S523-S530.  
[Crossref](#) | [Others](#)
- Agrawal, M., Pich, A., Zafeiropoulos, N.E., *et al.* Polystyrene-ZnO composite particles with controlled morphology. (2007) *Chem Mater* 19(7): S1845-S1852.  
[Crossref](#) | [Others](#)
- Chen, M., Hu, L., Xu, J., *et al.* ZnO Hollow-sphere nanofilm-based high-performance and low-cost photodetector. (2011) *Small* 7(17): S2449-S2453.  
[PubMed](#) | [Other](#)
- Zhou, J., Chen, M., Qiao, X., *et al.* Facile preparation method of SiO<sub>2</sub>/PS/TiO<sub>2</sub> multilayer core-shell hybrid microspheres. (2006) *Langmuir* 22(24): S10175-S10179.  
[PubMed](#) | [Crossref](#) | [Others](#)
- Yoshida, M., Prasad, P.N. Sol-gel-processed SiO<sub>2</sub>/TiO<sub>2</sub>/poly (vinylpyrrolidone) composite materials for optical waveguides. (1996) *Chem Mater* 8(1): S235-S241.  
[Crossref](#) | [Others](#)
- Kim, M.J., Chae, H.S., Choi, H.J. Core-shell structured poly(methyl methacrylate)-coated zirconium dioxide nanoparticle and its dispersion stability. (2015) *J Ind Eng Chem* 21(1): S145-S150.  
[Crossref](#) | [Others](#)
- Yi, D.K., Lee, S.S., Ying, J.Y. Synthesis and applications of magnetic nanocomposite catalysts. (2006) *Chem Mater* 18(10): S2459-S2461.  
[Crossref](#) | [Others](#)
- Roca, M., Haes, A.J. Silica-void-gold nanoparticles: temporally stable surface-enhanced Raman scattering substrates. (2008) *J Am Chem Soc* 130(43): S14273-S14279.  
[PubMed](#) | [Crossref](#) | [Others](#)
- Xu, H., Tong, N., Cui, L., *et al.* Preparation of hydrophilic magnetic nanospheres with high saturation magnetization. (2007) *J Magn Magn Mater* 311(1): S125-S130.  
[Crossref](#) | [Others](#)
- Halavaara, J., Tervahartiala, P., Isoniemi, H., *et al.* Efficacy of sequential use of superparamagnetic iron oxide and gadolinium in liver MR imaging. (2002) *Acta Radiol* 43(2): S180-S185.  
[PubMed](#) | [Crossref](#) | [Others](#)
- Lübbe, A.S., Alexiou, C., Bergemann, C. Clinical applications of magnetic drug targeting. (2001) *J Surg Res* 95(2): S200-S206.  
[PubMed](#) | [Crossref](#) | [Others](#)
- Kwon, S.H., Sim, B., Choi, H.J. Magnetorheological characteristics of nano-sized iron oxide coated polyaniline composites. (2016) *IEEE Trans Magn* 52(7): S1-S4.  
[Crossref](#) | [Others](#)
- Xu, X., Friedman, G., Humfeld, K.D., *et al.* Superparamagnetic photonic crystals. (2001) *Adv Mater* 13(22): S1681-S1684.  
[Others](#)
- Huang, Z.B., Tang, F.Q. Preparation, structure, and magnetic properties of polystyrene coated by Fe<sub>3</sub>O<sub>4</sub> nanoparticles. (2004) *J Colloid Interface Sci* 275(1): S142-S147.  
[PubMed](#) | [Crossref](#) | [Others](#)
- Huang, Z., Tang, F., Zhang, L. Morphology control and texture of Fe<sub>3</sub>O<sub>4</sub> nanoparticle-coated polystyrene microspheres by ethylene glycol in forced hydrolysis reaction. (2005) *Thin Solid Films* 471(1): S105-S112.  
[Crossref](#) | [Others](#)
- Fang, F.F., Kim, J.H., Choi, H.J. Synthesis of core-shell structured PS/Fe<sub>3</sub>O<sub>4</sub> microbeads and their magnetorheology. (2009) *Polym* 50(10): S2290-S2293.  
[Crossref](#) | [Others](#)
- Puentes-Vara, L.A., Gregorio-Jauregui, K.M., Bolarín, A.M., *et al.* Effects of surfactant and polymerization method on the synthesis of magnetic colloidal polymeric nanoparticles. (2016) *J Nanopart Res* 18(7): S212.  
[Crossref](#) | [Others](#)
- Yang, Y., Chu, Y., Yang, F., *et al.* Uniform hollow conductive polymer microspheres synthesized with the sulfonated polystyrene template. (2005) *Mater Chem Phys* 92(1): S164-S171.  
[Crossref](#) | [Others](#)
- Yu, S.H., Yoshimura, M. Shape and phase control of ZnS nanocrystals: template fabrication of wurtzite ZnS single-crystal nanosheets and ZnO flake-like dendrites from a lamellar molecular precursor ZnS•(N-H<sub>2</sub>CH<sub>2</sub>CH<sub>2</sub>NH<sub>2</sub>)<sub>0.5</sub>. (2002) *Adv Mater* 14(4): S296-S300.  
[Crossref](#) | [Others](#)
- Ismail, A.A., El-Midany, A., Abdel-Aal, E.A., *et al.* Application of statistical design to optimize the preparation of ZnO nanoparticles via hydrothermal technique. (2005) *Mater Lett* 59(14-15): S1924-S1928.  
[Crossref](#) | [Others](#)
- Xuan, S., Wang, F., Lai, J.M.Y., *et al.* Synthesis of biocompatible, mesoporous Fe<sub>3</sub>O<sub>4</sub> nano/microspheres with large surface area for magnetic resonance imaging and therapeutic applications. (2011) *ACS Appl Mat Interfaces* 3(2): S237-S244.  
[PubMed](#) | [Crossref](#) | [Others](#)